PLOS ONE

Generation of Interleukin-2 Receptor Gamma Gene Knockout Pigs from Somatic Cells Genetically Modified by Zinc Finger Nuclease-Encoding mRNA

Masahito Watanabe[1,2], Kazuaki Nakano[1], Hitomi Matsunari[1,2], Taisuke Matsuda[1], Miki Maehara[1], Takahiro Kanai[1], Mirina Kobayashi[1], Yukina Matsumura[1], Rieko Sakai[1], Momoko Kuramoto[1], Gota Hayashida[1], Yoshinori Asano[1], Shuko Takayanagi[1], Yoshikazu Arai[1], Kazuhiro Umeyama[1,2], Masaki Nagaya[2], Yutaka Hanazono[3,4], Hiroshi Nagashima[1,2,4]*

1 Laboratory of Developmental Engineering, Department of Life Sciences, School of Agriculture, Meiji University, Kawasaki, Japan, **2** Meiji University International Institute for Bio-Resource Research (MUIIBR), Kawasaki, Japan, **3** Division of Regenerative Medicine, Center for Molecular Medicine, Jichi Medical University, Tochigi, Japan, **4** CREST, Japan Science and Technology Agency, Tokyo, Japan

Abstract

Zinc finger nuclease (ZFN) is a powerful tool for genome editing. ZFN-encoding plasmid DNA expression systems have been recently employed for the generation of gene knockout (KO) pigs, although one major limitation of this technology is the use of potentially harmful genome-integrating plasmid DNAs. Here we describe a simple, non-integrating strategy for generating KO pigs using ZFN-encoding mRNA. The interleukin-2 receptor gamma (*IL2RG*) gene was knocked out in porcine fetal fibroblasts using ZFN-encoding mRNAs, and *IL2RG* KO pigs were subsequently generated using these KO cells through somatic cell nuclear transfer (SCNT). The resulting *IL2RG* KO pigs completely lacked a thymus and were deficient in T and NK cells, similar to human X-linked SCID patients. Our findings demonstrate that the combination of ZFN-encoding mRNAs and SCNT provides a simple robust method for producing KO pigs without genomic integration.

Citation: Watanabe M, Nakano K, Matsunari H, Matsuda T, Maehara M, et al. (2013) Generation of Interleukin-2 Receptor Gamma Gene Knockout Pigs from Somatic Cells Genetically Modified by Zinc Finger Nuclease-Encoding mRNA. PLoS ONE 8(10): e76478. doi:10.1371/journal.pone.0076478

Editor: Andrew C. Wilber, Southern Illinois University School of Medicine, United States of America

Received July 4, 2013; **Accepted** August 23, 2013; **Published** October 9, 2013

Funding: This work was supported by the Core Research for Evolutional Science and Technology (CREST) of the Japan Science and Technology Agency and by the Meiji University International Institute for Bio-Resource Research (MUIIBR). The funders had no role in study design, data collection and analysis, decision to publish, or preparation of the manuscript.

Competing Interests: The authors have declared that no competing interests exist.

* E-mail: hnagas@isc.meiji.ac.jp

Introduction

Pigs have attracted attention as large experimental animals capable of providing valuable information that is highly extrapolatable to humans due to their anatomical, physiological, and hematological features [1–5]. To date, pig models of various human diseases, such as cystic fibrosis [6], diabetes mellitus [7,8], Alzheimer's disease [9], and retinitis pigmentosa [10], have been created. In addition, research on the use of genetically modified pigs as organ/tissue donors for xenotransplantation into humans is advancing [11,12]. In fact, encapsulated porcine islets of Langerhans have been transplanted into humans and are now under clinical trials to assess their safety and efficacy for curing type I diabetes mellitus [13].

The knockout (KO) of endogenous genes is a useful tool for analyses of gene function and the production of animal models that mimic human diseases. A variety of gene KO mice have been generated using embryonic stem (ES) cells genetically modified by homologous recombination (HR). As authentic ES cells are not available in pigs, HR using somatic cells has been employed to generate gene KO pigs in combination with somatic cell nuclear transfer (SCNT) technology. However, the low efficiency (frequency, 10^{-6} to 10^{-8}) of HR for mammalian cultured cells hinders the generation of KO pigs [14–16], and the generation of KO pigs through HR therefore remains limited.

One new technique uses zinc finger nucleases (ZFNs) to knock out endogenous genes and is expected to overcome the inefficiency and complexity of HR in mammals [17]. Engineered ZFNs are artificial restriction enzymes comprised of a zinc finger DNA-binding domain and a DNA cleavage domain [18]. We previously were the first to demonstrate that gene KO in primary porcine fetal fibroblasts *in vitro* was possible using ZFNs [19], and somatic cells that were genetically modified by ZFNs were shown to be capable of producing gene KO pigs after SCNT [20–23]. In these studies, the ZFN-encoding plasmid DNA was introduced into somatic cells or the nuclear donor cells for SCNT. However, plasmid DNA can also be integrated into the genome of cells, which may result in the disruption of endogenous genes and the constitutive expression of ZFNs. This drawback of plasmid DNA can be eliminated by the use of ZFN-encoding mRNA, which cannot be inserted into the host genome. Gene KO using ZFN-encoding mRNAs in rodents has been performed via direct injection into the fertilized eggs [24–26], although the generation of KO piglets using ZFN-encoding mRNA has yet to be reported.

The present study sought to investigate whether ZFN-encoding mRNAs can be used to generate gene KO pigs. We chose the

interleukin-2 receptor gamma (*IL2RG*) gene on the X-chromosome of male cells as a target gene to be knocked out. *IL2RG* encodes the common gamma chain (γ_c), and mutations in *IL2RG* lead to X-linked severe combined immunodeficiency (XSCID), which is characterized by profound defects in cellular and humoral immunity in humans [27,28]. Furthermore, knockout of *IL2RG* was previously shown to give rise to the XSCID phenotype in male pigs [29]. We therefore applied ZFN-encoding mRNA to knock out *IL2RG* in male porcine fibroblast cells, which are capable of supporting the development to live offspring after SCNT. Here, we show that an endogenous gene in porcine primary cultured cells could be knocked out using ZFN-encoding mRNAs, thereby allowing the efficient production of a gene KO pig by means of somatic cell cloning.

Results

Design of ZFNs and isolation of *IL2RG* KO cells

Similar to *IL2RG* in humans, mice, and rats, porcine *IL2RG* is found on the X chromosome and consists of 8 exons [30]. In this study, we constructed a ZFN that targets exon 1 of porcine *IL2RG*. This pair (right and left) of ZFNs contains 4 zinc finger proteins each, and both the right and left ZFNs recognize a target sequence of 24 bp (Figure 1A). *IL2RG* KO cells were generated via the electroporation of ZFN-encoding mRNAs into porcine male fetal fibroblasts with transient cold shock treatment at 32°C for 3 d [31]. No visible morphological abnormalities were detected in the fetal fibroblasts following the introduction of mRNA and transient cold shock treatment. Of the 192 single cell-derived cell lines obtained by limiting dilution, 1 cell line (1/192, 0.5%) with a ZFN-induced mutation was established, and this cell line (#98, Figure 1B) was used as the nuclear donor for SCNT. DNA sequence analyses showed that these cells carried both a 3-bp substitution and an 86-bp deletion spanning the major transcription start point and the start codon (ATG) of porcine *IL2RG*, indicating that this mutation was likely to disrupt *IL2RG* function. Sufficient numbers of KO cells were prepared for SCNT after culture for 3 weeks.

Production and analysis of *IL2RG* KO cloned pigs

First, the developmental competence of the SCNT embryos reconstructed with the *IL2RG* KO cells was examined *in vitro*. Of the 403 SCNT embryos produced in duplicated experiments, 237 (58.8%) developed into blastocysts (Table 1). This blastocyst formation rate was comparable to those reported in our previous studies [32]. Second, 199 blastocysts (Figure 2A) obtained by SCNT were subjected to transfer to 2 estrus synchronized recipient gilts (P177 and P178; Table 1). Pregnancy was confirmed in both gilts at 39 d of gestation. On day 113 of gestation, 4 male cloned pigs were obtained from 1 recipient (P177) via cesarean section (Figure 2B). The body weight and length of the 4 piglets ranged from 0.56 to 1.16 kg and 22 to 28 cm, respectively. The other recipient (P178) miscarried at 46 d of gestation.

PCR genotyping and DNA sequence analyses of the 4 cloned pigs showed that all 4 pigs had the same mutation as the nuclear donor cells (3-bp substitution and 86-bp deletion; Figure 2C and D). Western blot analyses further showed that all 4 pigs lacked the IL2RG protein (Figure 2E).

Phenotypic characterization of *IL2RG* KO pigs

Gross anatomical analysis revealed that all 4 *IL2RG* KO pigs completely lacked thymuses (Figure 3A, B). Histological analysis of the spleens clearly showed the presence of lymphocytes in the white pulp of the peripheral lymphoid sheath tissue (PALS) in wild-type (WT) pigs (Figure 3C), whereas the *IL2RG* KO pigs showed very few or no lymphocytes in the PALS (Figure 3D). Embryonic hematopoiesis in the red pulp was strong in both WT and *IL2RG* KO pigs (data not shown). The lymphocyte counts in the peripheral blood of the WT and *IL2RG* KO pigs were $15.7\pm2.2\times10^2/\mu l$ and $6.5\pm3.0\times10^2/\mu l$, respectively, indicating a significant reduction in the lymphocyte number in *IL2RG* KO pigs ($P<0.01$; Figure 3E).

Flow cytometric analyses of the peripheral blood (Figure 4A) showed that the number of $CD3^+$ T cells in *IL2RG* KO pigs ($0.3\%\pm0.1\%$) was drastically lower than that in WT pigs ($74.0\%\pm10.2\%$; $P<0.0001$). In addition, *IL2RG* KO pigs lacked $CD3^+CD4^+$ and $CD3^+CD8^+$ T cells. The number of NK cells (monocyte/granulocyte$^-$, $CD3^-$, and $CD16^+$) was also notably lower in *IL2RG* KO pigs than WT pigs (*IL2RG* KO, $0.9\%\pm0.2\%$ vs. WT, $8.1\pm4.5\%$; $P=0.004$), although the B cell population ($CD3^-$ and $CD45RA^+$) in *IL2RG* KO pigs was observed to be the same as that in WT pigs. As observed in the peripheral blood, the numbers of splenic T cells (*IL2RG* KO, $0.2\%\pm0.1\%$ vs. WT, $28.1\%\pm10.9\%$; $P<0.0001$) and NK cells (*IL2RG* KO, $0.8\%\pm0.3\%$ vs. WT, $3.9\%\pm0.8\%$; $P=0.0001$) were significantly reduced in *IL2RG* KO pigs (Figure 4B). Thus, an almost complete lack of T and NK cells was observed in the *IL2RG* KO pigs, which is similar to human XSCID patients.

Discussion

In rodents, the microinjection of ZFN-encoding mRNA into fertilized eggs has been used for the creation of gene KO animals, mainly due to its simplicity. However, the drawbacks of this microinjection method include inefficiency and the occurrence of mutation mosaicism [24]. The transfer of mRNA-injected eggs into recipient females gives rise to both non-mutant and mutant offspring, and the generation of mutants results in undesired mutations that are meaningless with regard to the traits of the gene KO animals. Mutation mosaicism can result from sustained ZFN activity during later embryogenesis or the re-cleavage of the already-modified alleles [33,34]. Individuals with the desired mutation can be selected after crossbreeding with WT animals. Such a breeding process, however, requires enormous time, labor, and costs in large animals such as pigs, which have longer gestation intervals than rodents. We therefore applied the gene KO procedure using SCNT for the generation of *IL2RG* KO pigs in the present study. With this method, nuclear donor cells could be examined *in vitro* for the induced mutations prior to the production of cloned animals by SCNT [2]. Thus, the wasteful production of undesired animals can be avoided. To our knowledge, this study is the first to demonstrate the generation of cloned pigs from gene KO cells prepared using ZFN-encoding mRNA.

For the generation of gene KO pigs by somatic cell cloning, HR has traditionally been used to knock out a target gene in nuclear donor cells [11,12,29]. In HR, an antibiotic-based cell selection is performed to obtain KO cells; however, several issues arise, including (1) the insertion of an antibiotic cassette into the host genome using targeting vectors, (2) the senescence or exhaustion of nuclear donor cells caused by the prolonged culture associated with antibiotic selection, and (3) the unavoidable contamination of non-targeted cells despite the positive–negative screening [29,35–37]. Therefore, a re-cloning process, namely repeated nuclear transfer, is often necessary to obtain KO offspring [38,39]. In the re-cloning process, fetuses are collected after the first round of SCNT and embryo transfer, and these first-round cloned fetuses can be analyzed for gene KO status. The establishment of primary

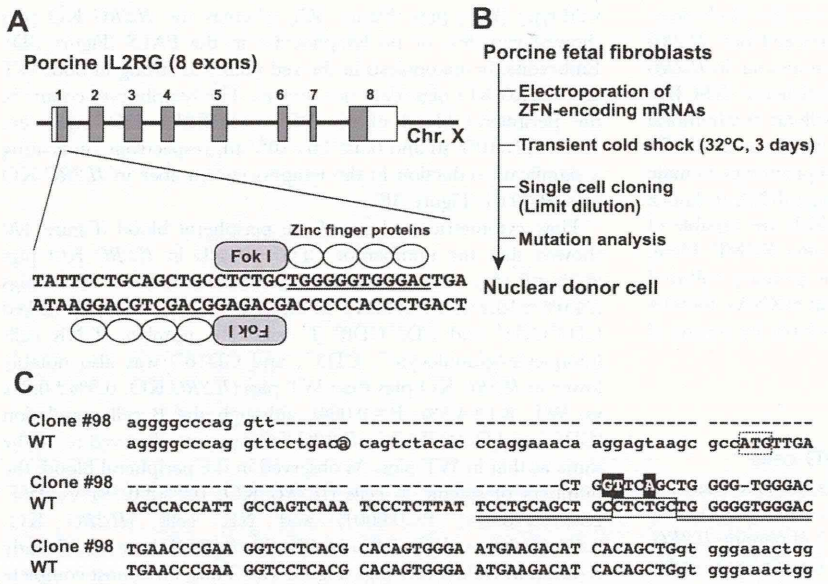

Figure 1. Design of ZFNs targeting the pig *IL2RG* gene and isolation of nuclear donor cells. (A) Schematic representation of ZFNs binding to pig *IL2RG*. The coding and untranslated regions are indicated by gray and white boxes, respectively. A ZFN consists of a nuclease domain (Fok I) and a DNA-binding domain (zinc finger proteins), and the recognition sequences of the zinc finger proteins are underlined. (B) Flow chart for the isolation of nuclear donor cells (clone #98) for SCNT. (C) ZFN-induced mutation in cell clone #98. The upper and lower sequences represent the WT and clone #98 sequence of *IL2RG*, respectively. The deletion mutation and nucleotide substitution in clone #98 are indicated by a hyphen and black box, respectively. The initiation codon of *IL2RG* is shown in a dotted box. The ZFN-binding and ZFN-cleavage sites are double-underlined and boxed, respectively. The major transcription initiation site is indicated with a circle.
doi:10.1371/journal.pone.0076478.g001

culture cells from the gene KO fetus requires obtaining rejuvenated nuclear donor cells for the next round of SCNT. Using these rejuvenated cells, the antibiotic cassette can be excised, provided that the proper site-specific recombinase technology, such as Cre-*lox*P recombination, was incorporated [40].

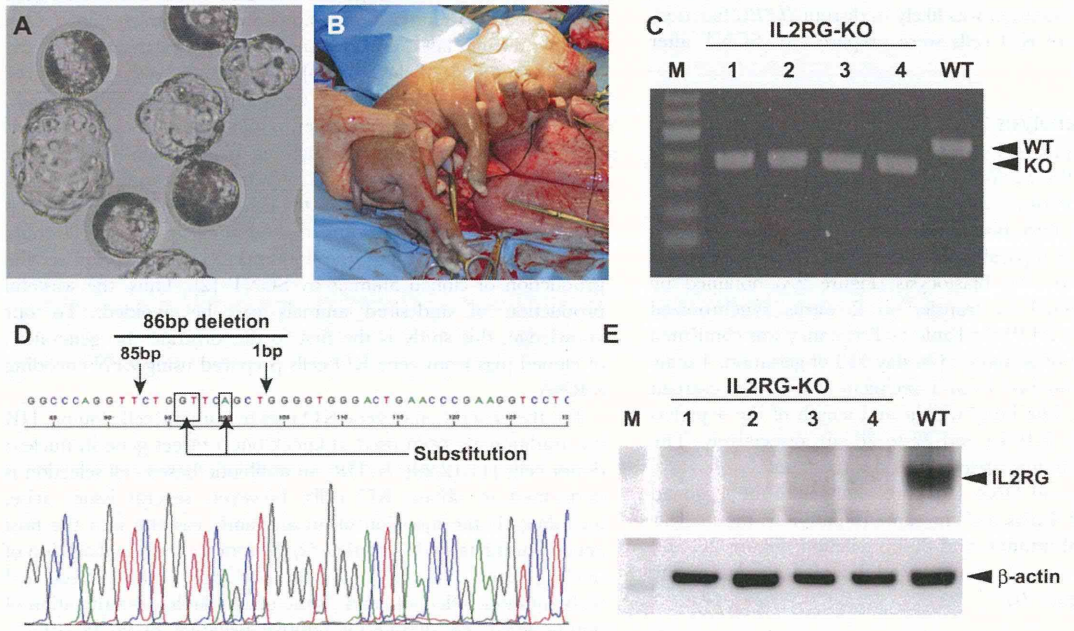

Figure 2. Generation and analysis of *IL2RG* KO pigs. (A) Cloned blastocysts transferred to recipient gilts. (B) Cloned *IL2RG* KO pig delivered by cesarean section at 113 d of gestation. (C) PCR genotyping for the 4 cloned piglets obtained. M: DNA marker. (D) The DNA sequence analysis of *IL2RG* in a cloned pig. The arrows and boxes indicate the same mutation as that of the nuclear donor cell (clone #98). (E) Western blot for IL2RG protein in the spleens of *IL2RG* KO pigs. β-actin was used as a loading control. M: protein standard marker.
doi:10.1371/journal.pone.0076478.g002

Table 1. *in vitro* development of SCNT embryos and production of *IL2RG* KO pigs.

in vitro development of reconstructed SCNT embryos		
SCNT embryos reconstructed	403	
Normally cleaved embryos on day 2	151 (71.9%)	
Blastocyst-stage embryos on day 5	237 (58.8%)	
Production of *IL2RG* KO pigs		
Recipient	P177	P178
Blastocysts transferred[a]	100	99
Pregnancy	+	+
Cloned fetuses obtained	4 (4.0%)	- (miscarried)[b]

[a]Day 5–6 embryos.
[b]46 d of gestation.
doi:10.1371/journal.pone.0076478.t001

In contrast, ZFN-encoding mRNAs can generate gene KO cells without antibiotic selection. In fact, sufficient numbers of nuclear donor cells for SCNT can be obtained in a short period of time (approximately 3 weeks). Moreover, the *IL2RG*-KO cells generated by the ZFN-encoding mRNAs in this study allowed for the direct production of full-term cloned fetuses without rejuvenation of the nuclear donor cells and subsequent re-cloning. As a result, we obtained full-term cloned fetuses within 6 months, including the period spent establishing the KO cells, whereas the HR method requires an average of 12 to 18 months to obtain KO animals. An additional advantage of ZFN-encoding mRNAs is transient ZFN expression, which reduces the incidence of off-target mutations [41]. Off-target events are a potential limitation of the ZFN technique [26,42,43], although the introduction of ZFN-encoding mRNAs leads to the immediate translation of ZFNs in the cytoplasm without the risk of genomic integration, which could disrupt endogenous genes. Carlson et al. recently generated KO pigs using TALEN-encoding mRNA [44]. Based on these collective results, we believe that it is important to compare the efficiencies of ZFN- and TALEN-mRNA in generating KO pigs.

A marked decrease in the number of T and B cells has been reported in XSCID mice [45,46] and rats [24]. In human XSCID patients, although the number of T and NK cells is significantly decreased, the number of B cells remains normal or is occasionally increased [28,47]. Thus, the phenotypes of rodent XSCID models do not necessarily mimic the conditions of human XSCID. In contrast, the *IL2RG* KO pigs obtained in this study lacked T and NK cells but showed normal B cell populations, and identical phenotypic characteristics were shown in a previous report in which XSCID pigs were generated through HR [29]. Thus, *IL2RG* KO pigs are considered to be an accurate model that mimics human XSCID.

Opportunistic infections in XSCID animals after birth are unavoidable under conventional housing conditions. We therefore used the full-term *IL2RG* KO pig fetuses recovered via cesarean section (113 d of gestation) for our analyses to avoid any changes due to infections.

In conclusion, this study presents a simple, non-integrating strategy for generating KO pigs using ZFN-encoding mRNA, which successfully generated *IL2RG* KO pigs via the SCNT method in a short period of time. The combination of ZFN-encoding mRNA with SCNT provides a robust method for generating KO pigs without genomic integration. Moreover, the resulting *IL2RG* KO pigs showed a phenotype similar to that of human XSCID. Although further characterization is required, these findings represent the first step toward developing a porcine SCID model, and we believe that this *IL2RG* KO pig model will greatly contribute not only to cancer and stem cell research but also to preclinical evaluations of the transplantation of pluripotent stem cells, such as iPS cells.

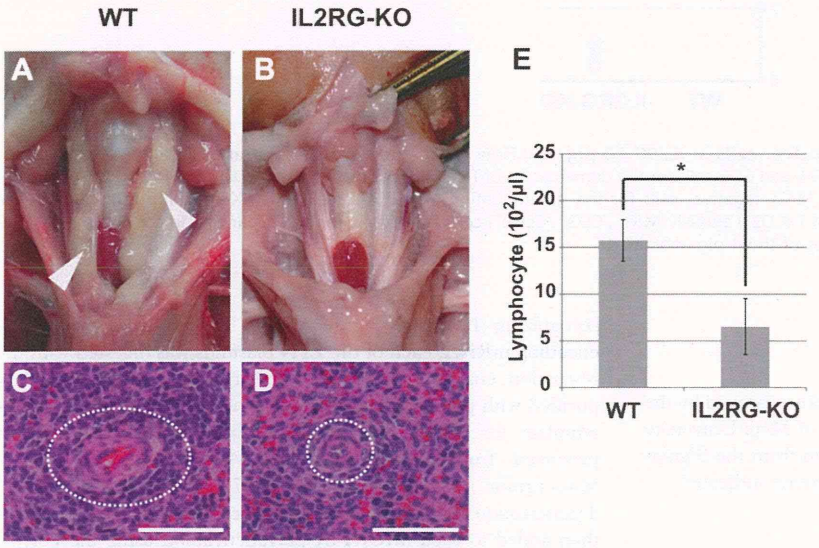

Figure 3. Phenotypes of *IL2RG* KO pigs. (A, B) The thymic phenotype in WT and *IL2RG* KO pigs. The white arrowheads indicate normal thymuses in WT pigs. (C, D) Histological analysis of the spleens of WT and *IL2RG* KO pigs. The white pulp of the spleen is indicated by a dotted white circle. Bar = 100 μm. (E) The proportion of lymphocytes in the peripheral blood (PB) of WT and *IL2RG* KO pigs. The data represent the means ± SD values for 4 pigs. The asterisk indicates a statistically significant difference ($P<0.01$) between the values for WT and *IL2RG* KO pigs (n = 4).
doi:10.1371/journal.pone.0076478.g003

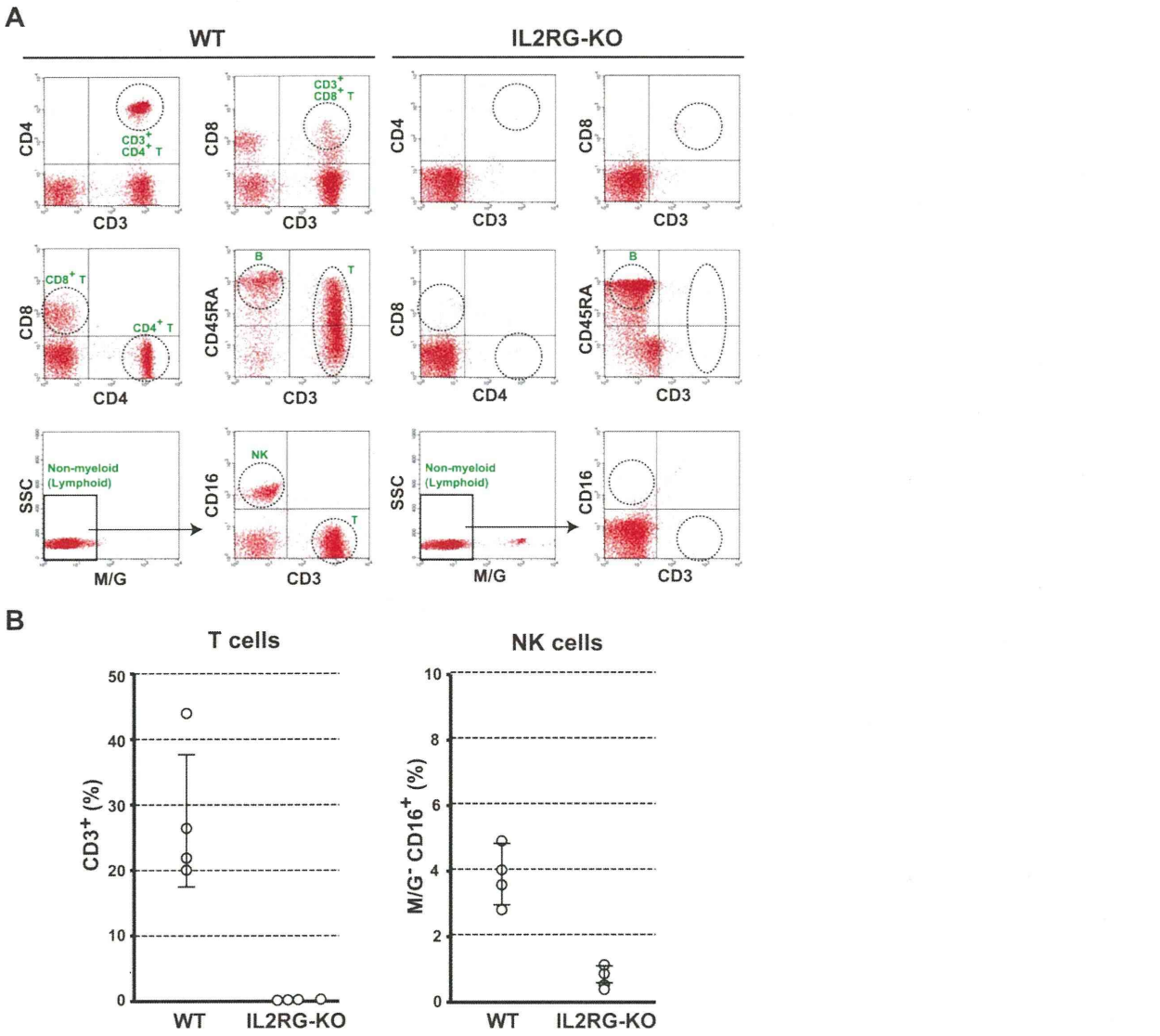

Figure 4. Flow cytometric analysis of mononuclear cells in *IL2RG* KO pigs. (A) Flow cytometric analysis of T, B, and NK cells in the peripheral blood of *IL2RG* KO pigs. The dot plots show CD3, CD4, and CD8 cells for the demarcation of T cell subpopulations and CD3, CD45RA, and CD16 (in the non-myeloid fraction, i.e., monocyte/granulocyte (M/G)-negative) cells for the differentiation of T cell, B cell, and NK cell subpopulations in the peripheral blood, respectively. (B) The proportion of T ($CD3^+$) and NK (M/G^-, $CD3^-$, $CD16^+$) cells among the mononuclear cells in the spleens of *IL2RG* KO pigs. The data represent the mean ± SD values of the 4 pigs obtained.
doi:10.1371/journal.pone.0076478.g004

Materials and Methods

Animal care and chemicals

All of the animal experiments in this study were approved by the Institutional Animal Care and Use Committee of Meiji University (IACUC10-0004). All chemicals were purchased from the Sigma-Aldrich Chemical Co. (MO, USA) unless otherwise indicated.

Design of ZFNs and mRNA preparation

Custom ZFN plasmids for pig *IL2RG* were obtained from Toolgen Inc. The design and validation of these ZFNs was performed by Toolgen Inc (Seoul, South Korea). The constructed ZFNs were designed to target the sequence of exon 1 in the pig *IL2RG* gene. Each of the ZFNs had 4 zinc finger domains recognizing 12 bases (Figure 1). For the production of ZFN-encoding mRNA, each of the ZFN plasmids was digested with the restriction enzyme Xho I. The linearized plasmids were then purified with phenol/chloroform to generate a high-quality DNA template for *in vitro* transcription. Capped ZFN mRNA was produced from the linearized DNA template via *in vitro* transcription using a MessageMAX T7 ARCA-Capped Message Transcription Kit (Cambio, Cambridge, UK). A poly(A) tail was then added to each mRNA by polyadenylation using the Poly(A) Polymerase Tailing Kit (Cambio). The poly(A)-tailed ZFN-encoding mRNA was then purified using a spin column with the MEGAclear Kit (Life Technologies, CA, USA) and finally resuspended in RNase-free water at 400 ng/ μl.

Isolation of *IL2RG* KO cells and culture conditions

A primary culture of porcine fetal fibroblast cells (male line) was used as the progenitor line for the isolation of *IL2RG* KO cells. The fibroblast cells and their derivatives (KO cells) were seeded onto type I collagen-coated dishes or plates (Asahi Glass, Tokyo, Japan) and cultured in MEMα (Life Technologies) supplemented with 15% FBS (Nichirei Bioscience, Tokyo, Japan) and 1× antibiotic-antimycotic solution (Life Technologies) in a humidified atmosphere containing 5% CO_2 at 37°C. The fetal fibroblasts were cultured to 70–90% confluence, washed twice with D-PBS(−) (Life Technologies), and treated with 0.05% trypsin-EDTA (Life Technologies) to isolate and collect the cells. The cells (4×10^5) were then suspended in 40 µl of R buffer (supplied as part of the Neon Transfection System, Life Technologies), and 2 µl of ZFN-encoding mRNA solution (400 ng/ µl) was added. The cells were then electroporated under the following conditions: pulse voltage, 1,100 V; pulse width, 30 ms; and pulse number, 1 (program #6). Following electroporation, the cells were cultured at 32°C for 3 d (transient cold shock) first without antibiotics in the medium described above for 24 h and then with antibiotics in the medium [31]. For recovery after the transient cold shock treatment, the cells were cultured at 37°C until they approached confluence, and then limiting dilution was performed to obtain single cell-derived clones in five 96-well plates. At 12 d after limiting dilution, cells at relatively high confluency (>50%) in each well were selected and divided for further culture and mutation analysis. The cells at low confluency (~50%) after limiting dilution were not used in further experiments.

Analysis of ZFN-induced mutations in nuclear donor cells and cloned fetuses

The target region of IL2RG-ZFNs was amplified by direct PCR from the cell clones using MightyAmp DNA polymerase (Takara Bio, Shiga, Japan) and the corresponding primers (5′-ATAGTGGTGTCAGTGTGATTGAGC and 5′-TACGAACT-GACTTATGACTTACC). Nested PCR was then performed using PrimeSTAR HS DNA polymerase (Takara Bio) and the appropriate primers (5′-ATACCCAGCTTTCGTCTCTGC and 5′-TTCCAGAATTCTATACGACC). Subsequently, the PCR fragment including the ZFN target region was examined using the sequencing primer 5′-AGCCTGTGTCATAGCATAC, the BigDye Terminator Cycle Sequencing Kit, and an ABI PRISM 3100 Genetic Analyzer (Life Technologies). For analysis of the mutation in cloned fetuses, genomic DNA was extracted from the tail biopsies of fetuses using a DNeasy Tissue and Blood Kit (QIAGEN, Hilden, Germany), and then PCR genotyping and DNA sequencing were performed as described above. All new sequence data is deposited in DDBJ/EMBL/GenBank (AB846644-AB846648).

SCNT and embryo transfer

SCNT was performed as described previously with slight modifications [32]. Briefly, *in vitro*-matured oocytes containing the first polar body were enucleated via the gentle aspiration of the polar body and the adjacent cytoplasm using a beveled pipette in 10 mM HEPES-buffered Tyrode lactose medium containing 0.3% (w/v) polyvinylpyrrolidone (PVP), 0.1 µg/ml demecolcine, 5 µg/ml cytochalasin B (CB), and 10% FBS. Fibroblasts (clone #98) were used as nuclear donors following cell cycle synchronization via serum starvation for 2 d. A single donor cell was inserted into the perivitelline space of an enucleated oocyte. The donor cell-oocyte complexes were placed in a solution of 280 mM mannitol (Nacalai Tesque, Kyoto, Japan) (pH 7.2) containing 0.15 mM $MgSO_4$, 0.01% (w/v) PVA, and 0.5 mM HEPES and were held between 2 electrode needles. Membrane fusion was induced with a somatic hybridizer (LF201; NEPA GENE, Chiba, Japan) by applying a single direct-current (DC) pulse (200 V/mm, 20 µs) and a pre- and post-pulse alternating current (AC) field of 5 V at 1 MHz for 5 s. The reconstructed embryos were cultured in NCSU23 medium supplemented with 4 mg/ml BSA for 1 to 1.5 h, followed by electrical activation. The reconstructed embryos were then washed twice in an activation solution containing 280 mM mannitol, 0.05 mM $CaCl_2$, 0.1 mM $MgSO_4$, and 0.01% (w/v) PVA and were aligned between 2 wire electrodes (1.0 mm apart) of a fusion chamber slide filled with the activation solution. A single DC pulse of 150 V/mm was applied for 100 µs using an electrical pulsing machine (Multiporator; Eppendorf, Hamburg, Germany). After activation, the reconstructed embryos were transferred into PZM5 supplemented with 5 µg/ml CB and 500 nM Scriptaid for 3 h. The embryos were then transferred into PZM5 supplemented with Scriptaid and further cultured for 12 to 14 h. After incubation, the embryos were further cultured in PZM5, and the dish was maintained under a humidified atmosphere of 5% CO_2, 5% O_2, and 90% N_2 at 38.5°C. Beyond the morula stage, the embryos were cultured in PZM5 supplemented with 10% FBS.

Crossbred (Large White/Landrace × Duroc) prepubertal gilts weighing 100 to 105 kg were used as recipients of the SCNT embryos. The gilts were given a single intramuscular injection of 1,000 IU of eCG to induce estrus. Ovulation was induced by an intramuscular injection of 1,500 IU of hCG (Kawasaki Pharmaceutical, Kanagawa, Japan) that was given 66 h after the injection of eCG. The SCNT embryos cultured for 5 to 6 d were surgically transferred into the oviducts of the recipients approximately 146 h after hCG injection.

Western blot analysis

After the *IL2RG* KO and age-matched WT pigs were sacrificed, their dissected spleens were homogenized in RIPA buffer (Thermo Scientific, MA, USA) with a protease inhibitor cocktail (Nacalai Tesque) and subjected to centrifugation, and the supernatants were collected. The protein concentrations of the samples were quantified using a DC protein assay (Bio-Rad, CA, USA) based on the Lowry method. Approximately 40 µg of protein from the spleen extracts was subjected to 10% SDS-PAGE and transferred by electroblotting to a Hybond-P PVDF membrane (GE Healthcare Bio-Sciences, NJ, USA). The membranes were blocked for 30 min at room temperature with Blocking One (Nacalai Tesque). After blocking, the membranes were incubated with an anti-IL2RG antibody (1:200 dilution; Santa Cruz Biotechnology, CA, USA) for 1 h at room temperature and were subsequently incubated with HRP-conjugated anti-rabbit IgG antibody (1:5,000 dilution; Santa Cruz Biotechnology) for 1 h at room temperature. The blot was developed using ECL Western Blotting Detection Reagents (GE Healthcare Bio-Sciences). The signal was detected and imaged with an ImageQuant LAS-4000 system (GE Healthcare Bio-Sciences).

Flow cytometric analysis

Peripheral blood mononuclear cells were harvested from the whole blood and spleens of *IL2RG* KO pigs using the erythrocyte lysis solution PharmLyse (Becton Dickinson, BD, NJ, USA), and 1×10^6 cells were incubated with mouse anti-pig CD3e (Abcam, Cambridge, UK), CD4a (BD), CD8a (BD), CD16 (AbDSerotec, NC, USA), CD45RA (AbDSerotec), and monocyte and granulocyte (M/G, Abcam) antibodies for 30 min at room temperature. After incubation, the cell suspension was washed and resuspended

with PBS (−) supplemented with 1% FBS (w/v). The cell populations isolated from the peripheral blood and spleens of *IL2RG*-KO pigs were evaluated using a FACSCalibur flow cytometer (BD) equipped with a 488-nm argon laser. The cell debris and aggregates were gated out of the analysis using bivariate, forward/side scatter (FSC/SSC) parameters. In all analyses, the virtual lymphocyte population was gated, and the gated 1×10^4 events per sample were acquired and analyzed using CELLQuest Pro software (BD).

Histological analysis

After the *IL2RG* KO and age-matched WT pigs were sacrificed, their dissected spleens were fixed in 10% neutral buffered formalin solution (Wako Pure Chemical Industries, Osaka, Japan), embedded in paraffin, sectioned, and stained with hematoxylin and eosin using standard methods.

Acknowledgments

We acknowledge Mr. Hiroshi Kadoi (Kadoi Ltd.) for technical help.

Author Contributions

Conceived and designed the experiments: HN. Performed the experiments: MW KN HM TM MM TK M. Kobayashi YM RS M. Kuramoto GH Y. Asano ST Y. Arai. Analyzed the data: MW KN KU. Wrote the paper: MW MN HN. Final approval of the manuscript: MN YH HN.

References

1. Aigner B, Renner S, Kessler B, Klymiuk N, Kurome M, et al. (2010) Transgenic pigs as models for translational biomedical research. J Mol Med 88: 653–664.
2. Kues WA, Niemann H (2004) The contribution of farm animals to human health. Trends Biotechnol 22: 286–294.
3. Vajta G, Gjerris M (2006) Science and technology of farm animal cloning: state of the art. Anim Reprod Sci 92: 211–230.
4. Lunney JK (2007) Advances in swine biomedical model genomics. Int J Biol Sci 3: 179–184.
5. Matsunari H, Nagashima H (2009) Application of genetically modified and cloned pigs in translational research. J Reprod Dev 55: 225–230.
6. Rogers CS, Stoltz DA, Meyerholz DK, Ostedgaard LS, Rokhlina T, et al. (2008) Disruption of the CFTR gene produces a model of cystic fibrosis in newborn pigs. Science 321: 1837–1841.
7. Umeyama K, Watanabe M, Saito H, Kurome M, Tohi S, et al. (2009) Dominant-negative mutant hepatocyte nuclear factor 1alpha induces diabetes in transgenic-cloned pigs. Transgenic Res 18: 697–706.
8. Renner S, Fehlings C, Herbach N, Hofmann A, von Waldthausen DC, et al. (2010) Glucose intolerance and reduced proliferation of pancreatic beta-cells in transgenic pigs with impaired glucose-dependent insulinotropic polypeptide function. Diabetes 59: 1228–1238.
9. Kragh PM, Nielsen AL, Li J, Du Y, Lin L, et al. (2009) Hemizygous minipigs produced by random gene insertion and handmade cloning express the Alzheimer's disease-causing dominant mutation APPsw. Transgenic Res 18: 545–558.
10. Ross JW, Fernandez de Castro JP, Zhao J, Samuel M, Walters E, et al. (2012) Generation of an inbred miniature pig model of retinitis pigmentosa. Invest Ophthalmol Vis Sci 53: 501–507.
11. Dai Y, Vaught TD, Boone J, Chen SH, Phelps CJ, et al. (2002) Targeted disruption of the alpha1,3-galactosyltransferase gene in cloned pigs. Nat Biotechnol 20: 251–255.
12. Lai L, Kolber-Simonds D, Park KW, Cheong HT, Greenstein JL, et al. (2002) Production of alpha-1,3-galactosyltransferase knockout pigs by nuclear transfer cloning. Science 295: 1089–1092.
13. Elliott RB, Escobar L, Tan PL, Muzina M, Zwain S, et al. (2007) Live encapsulated porcine islets from a type 1 diabetic patient 9.5 yr after xenotransplantation. Xenotransplantation 14: 157–161.
14. Porter AC, Itzhaki JE (1993) Gene targeting in human somatic cells. Complete inactivation of an interferon-inducible gene. Eur J Biochem 218: 273–281.
15. Brown JP, Wei W, Sedivy JM (1997) Bypass of senescence after disruption of p21CIP1/WAF1 gene in normal diploid human fibroblasts. Science 277: 831–834.
16. van Nierop GP, de Vries AA, Holkers M, Vrijsen KR, Goncalves MA (2009) Stimulation of homology-directed gene targeting at an endogenous human locus by a nicking endonuclease. Nucleic Acids Res 37: 5725–5736.
17. Geurts AM, Cost GJ, Freyvert Y, Zeitler B, Miller JC, et al. (2009) Knockout rats via embryo microinjection of zinc-finger nucleases. Science 325: 433.
18. Kim YG, Cha J, Chandrasegaran S (1996) Hybrid restriction enzymes: zinc finger fusions to Fok I cleavage domain. Proc Natl Acad Sci U S A 93: 1156–1160.
19. Watanabe M, Umeyama K, Matsunari H, Takayanagi S, Haruyama E, et al. (2010) Knockout of exogenous EGFP gene in porcine somatic cells using zinc-finger nucleases. Biochem Biophys Res Commun 402: 14–18.
20. Whyte JJ, Zhao J, Wells KD, Samuel MS, Whitworth KM, et al. (2011) Gene targeting with zinc finger nucleases to produce cloned eGFP knockout pigs. Mol Reprod Dev 78: 2.
21. Hauschild J, Petersen B, Santiago Y, Queisser AL, Carnwath JW, et al. (2011) Efficient generation of a biallelic knockout in pigs using zinc-finger nucleases. Proc Natl Acad Sci U S A 108: 12013–12017.
22. Li P, Estrada JL, Burlak C, Tector AJ (2012) Biallelic knockout of the alpha-1,3 galactosyltransferase gene in porcine liver-derived cells using zinc finger nucleases. J Surg Res 181: e39–45.
23. Yang D, Yang H, Li W, Zhao B, Ouyang Z, et al. (2011) Generation of PPARgamma mono-allelic knockout pigs via zinc-finger nucleases and nuclear transfer cloning. Cell Res 21: 979–982.
24. Mashimo T, Takizawa A, Voigt B, Yoshimi K, Hiai H, et al. (2010) Generation of knockout rats with X-linked severe combined immunodeficiency (X-SCID) using zinc-finger nucleases. PLoS One 5: e8870.
25. Carbery ID, Ji D, Harrington A, Brown V, Weinstein EJ, et al. (2010) Targeted genome modification in mice using zinc-finger nucleases. Genetics 186: 451–459.
26. Cui X, Ji D, Fisher DA, Wu Y, Briner DM, et al. (2011) Targeted integration in rat and mouse embryos with zinc-finger nucleases. Nat Biotechnol 29: 64–67.
27. Noguchi M, Yi H, Rosenblatt HM, Filipovich AH, Adelstein S, et al. (1993) Interleukin-2 receptor gamma chain mutation results in X-linked severe combined immunodeficiency in humans. Cell 73: 147–157.
28. Buckley RH (2004) Molecular defects in human severe combined immunodeficiency and approaches to immune reconstitution. Annu Rev Immunol 22: 625–655.
29. Suzuki S, Iwamoto M, Saito Y, Fuchimoto D, Sembon S, et al. (2012) Il2rg Gene-Targeted Severe Combined Immunodeficiency Pigs. Cell Stem Cell 10: 753–758.
30. Honma D, Uenishi H, Hiraiwa H, Watanabe S, Tang W, et al. (2003) Cloning and characterization of porcine common gamma chain gene. J Interferon Cytokine Res 23: 101–111.
31. Doyon Y, Choi VM, Xia DF, Vo TD, Gregory PD, et al. (2010) Transient cold shock enhances zinc-finger nuclease-mediated gene disruption. Nat Methods 7: 459–460.
32. Matsunari H, Watanabe M, Umeyama K, Nakano K, Ikezawa Y, et al. (2012) Cloning of homozygous α1,3-galactosyltransferase gene knock-out pigs by somatic cell nuclear transfer. In: Miyagawa S, editor.Xenotransplantation. Rijeka, Croatia: InTech. pp. 37–54.
33. Tesson L, Usal C, Menoret S, Leung E, Niles BJ, et al. (2011) Knockout rats generated by embryo microinjection of TALENs. Nat Biotechnol 29: 695–696.
34. Sung YH, Baek IJ, Kim DH, Jeon J, Lee J, et al. (2013) Knockout mice created by TALEN-mediated gene targeting. Nat Biotechnol 31: 23–24.
35. Forsberg EJ, Strelchenko NS, Augenstein ML, Betthauser JM, Childs LA, et al. (2002) Production of cloned cattle from in vitro systems. Biol Reprod 67: 327–333.
36. Iguma LT, Lisauskas SF, Melo EO, Franco MM, Pivato I, et al. (2005) Development of bovine embryos reconstructed by nuclear transfer of transfected and non-transfected adult fibroblast cells. Genet Mol Res 4: 55–66.
37. Zakhartchenko V, Mueller S, Alberio R, Schernthaner W, Stojkovic M, et al. (2001) Nuclear transfer in cattle with non-transfected and transfected fetal or cloned transgenic fetal and postnatal fibroblasts. Mol Reprod Dev 60: 362–369.
38. Matsunari H, Onodera M, Tada N, Mochizuki H, Karasawa S, et al. (2008) Transgenic-cloned pigs systemically expressing red fluorescent protein, Kusabira-Orange. Cloning Stem Cells 10: 313–323.
39. Fujimura T, Murakami H, Kurome M, Takahagi Y, Shigehisa T, et al. (2008) Effects of recloning on the efficiency of production of alpha 1,3-galactosyltransferase knockout pigs. J Reprod Dev 54: 58–62.
40. Sternberg N, Hamilton D (1981) Bacteriophage P1 site-specific recombination. I. Recombination between loxP sites. J Mol Biol 150: 467–486.
41. Whyte JJ, Prather RS (2012) Cell Biology Symposium: Zinc finger nucleases to create custom-designed modifications in the swine (Sus scrofa) genome. J Anim Sci 90: 1111–1117.
42. Miller JC, Holmes MC, Wang J, Guschin DY, Lee YL, et al. (2007) An improved zinc-finger nuclease architecture for highly specific genome editing. Nat Biotechnol 25: 778–785.
43. Szczepek M, Brondani V, Buchel J, Serrano L, Segal DJ, et al. (2007) Structure-based redesign of the dimerization interface reduces the toxicity of zinc-finger nucleases. Nat Biotechnol 25: 786–793.
44. Carlson DF, Tan W, Lillico SG, Stverakova D, Proudfoot C, et al. (2012) Efficient TALEN-mediated gene knockoutnin livestock. Proc Natl Acad Sci U S A 109: 17382–17387.

45. Cao X, Shores EW, Hu-Li J, Anver MR, Kelsall BL, et al. (1995) Defective lymphoid development in mice lacking expression of the common cytokine receptor gamma chain. Immunity 2: 223–238.
46. DiSanto JP, Muller W, Guy-Grand D, Fischer A, Rajewsky K (1995) Lymphoid development in mice with a targeted deletion of the interleukin 2 receptor gamma chain. Proc Natl Acad Sci U S A 92: 377–381.
47. Sugamura K, Asao H, Kondo M, Tanaka N, Ishii N, et al. (1996) The interleukin-2 receptor gamma chain: its role in the multiple cytokine receptor complexes and T cell development in XSCID. Annu Rev Immunol 14: 179–205.

血栓止血誌 24(4) : 396～401, 2013

◆2013年度日本血栓止血学会　学術奨励賞◆

生体分子イメージングによる血栓の可視化

西村　智[*1,2]

In vivo imaging and thrombus formation

Satoshi NISHIMURA[*1,2]

◇要旨◇

生体でもっとも小さく核を有さない血小板は，一方で，多彩な生理作用を持つ．しかし，従来の手法では，単一血小板は生体内で可視化することができず，生体での機能にも不明な点が多かった．我々は，一光子共焦点・二光子レーザー顕微鏡を用いた「生体分子イメージング手法」を独自に開発し，血栓症をはじめとする生活習慣病にアプローチしてきた．本手法を用いて生体内の血栓形成過程の詳細も明らかになり，iPS由来の人工血小板の機能解析も可能となっている．生体内での血小板の活性化機構と血栓止血機能，さらに多彩な生命生理現象との関わりに対して，新規アプローチを中心に紹介する．

Key words: 生体分子イメージング，血栓，血小板，慢性炎症，肥満脂肪組織

1．はじめに　生体イメージングとは

最近の研究により，心筋梗塞や脳卒中などの原因となるメタボリックシンドロームと慢性炎症病態に密接な関連があることが示唆されている．メタボリックシンドロームでは，遺伝子素因と，内蔵肥満・加齢・喫煙などの外的誘因の両者が病態形成に関わっていることは，多くの臨床データから明らかである．しかし，慢性炎症そのものの動態が不明であることから，基礎病態に対する特効薬的な治療が存在せず，それに伴う生活習慣病病態については，多くの有疾患患者と高い死亡率を生んでいるのが現状である．そして，病態理解のためには，慢性炎症に伴う生体内での細胞動態の異常，特に免疫細胞の局所での生体内応答について，直接画像化して知見を得ることは必須であると言える．

我々は，独自に開発した「生体分子イメージング手法」を，まず，肥満した脂肪組織に適応し，メタボリックシンドロームの病態にアプローチを行ってきた．本稿では，我々の生体イメージングより明らかになった，血栓形成過程についての知見を紹介したい．

2．生体内の組織の可視化　生体分子イメージングの開発

動脈硬化のように血管が主な傷害の場になる病態だけでなく，血栓症，腫瘍やメタボリックシンドロームにおいても，血流や血管機能といった生体内のダイナミックな変化，組織学的変化に先行

[*1] 東京大学医学系研究科循環器内科〔〒113-0853 東京都文京区本郷7-3-1〕
Department of Cardiovascular Medicine, The University of Tokyo
[*2] 東京大学システム疾患生命科学による先端医療技術開発拠点特任准教授
Translational Systems Biology and Medicine Initiative, The University of Tokyo
〔7-3-1, Hongo, Bunkyo-ku, Tokyo 123-0853, Japan〕
Tel: 03-3815-5411　Fax: 03-3814-0021　e-mail: snishi-tky@umin.ac.jp

する初期の炎症性変化を捉えることが可能な生体内分子イメージング技術は非常に有用である．従来の生体内観察では，透過光による観察が容易な腸間膜の微小循環を用いた研究が主に行われてきたが，近年の光学観察系・蛍光プローブの開発により，蛍光物質をトレーサーとして，透過光観察が不可能な厚みを有する脂肪組織をはじめとする実質臓器の血流観察も可能となった（**図1**）[1]．時間・空間解像度も飛躍的に改善し，細胞内小器官レベルでの解析が可能となっている．また後述の通り高速マルチカラー二光子生体イメージングも簡便に行われるようになっている．

3．組織イメージング手法 方法論を中心として

新たに開発した「生体分子イメージング」手法を概説する．現在，光学機器の進歩に伴い，高速レーザー共焦点顕微鏡を用いて，血流の方向と平行にごく狭い断面に焦点を合わせて画像取得し，高速に血管内を変形しながら流れる赤血球・白血球・血小板に各々フォーカスを合わせて観察が可能となった（**図1, 2**）．血管内の細胞動態を明らかにするために，我々は主に多数のピンホールを有する円盤を高速回転させて画像を取得するニポウ式の共焦点ユニット（横河電機，CSU X1），及び，シングルビームで組織をスキャンするレゾナンス型高速共焦点システム（Nikon A1R）を組み合わせて用いることにより，高速イメージングを行っている．我々のシステムでは，空間解像度はほぼ回折限界（光を用いて観察する際に，理論上，最大で得られる解像度が決まっている）に既に達しており，フルフレーム（512×512 ピクセル）で毎秒 30 コマ，最大 4 色の画像取得が可能である．二光子による画像取得では生体深部の画像も取得可能であり，骨髄内の細胞動態（巨核球からの血小板放出，幹細胞の動態）などの可視化にも成功している．

画像取得に際して，検体の準備としては，麻酔下のマウスに蛍光色素を静脈全身投与し，観察部位を切開・露出する．観察部位を生理食塩水により湿潤した後，観察窓を設け，マウスを倒立顕微鏡上において蛍光観察を行う．観察中はヒーティングプレートを用いて体温を 37 度に保つ．本手法により臓器表面から一光子では 50 から 100 ミクロン程度，二光子では最大 1mm の深部で細胞構築・血流が明瞭に観察可能である．トレーサーとしては，血流は蛍光物質 FITC デキストランを尾静脈から全身投与することにより可視化される．分子量 150,000 程度のデキストランは血管外に漏出することはなく，血管内にとどまり血球成分を可視化される．我々の観察では赤血球のみならず，毛細血管網を変形しながら流れる直径 2 ミクロン程度の血小板が明瞭に可視化されている．一方，分子量 7000 程度のデキストランはすみやかに間質に移行し，中間サイズの分子量の蛍光デキストランを用いて血管透過性を評価することも可能である．白血球は，ヘキスト，アクリジンオレンジ及びローダミンといった核染色色素を静脈投与し可視化される．いずれの色素も，毒性の無い投与量で，十分明るく生体内の細胞の核を明るく標識される．さらに，細胞表面マーカーに応じた蛍光標識抗体を用いることにより，特定細胞集団を生体内でも標識することが可能である．例えば，血小板に特異的な蛍光標識抗 CD41 抗体，抗 GPIb 抗体を全身投与することにより単一血小板も生体内で初めて可視化されている（後述）．血管内皮に対しては，血管内皮表面の糖鎖に特異的に結合する蛍光標識レクチンを用いることで，生体内で血管系を明瞭に描出することが可能である．そして，本分子イメージング手法は脂肪組織だけでなく，骨格筋・肝臓・腎臓（糸球体を含む）・腸管（絨毛レベルまで）など，さまざま実質臓器に応用可能であり，臓器血流・細胞動態を観察・定量することも可能になっている．

4．血小板機能の生体イメージングを用いた可視化

本邦の死因の上位を占める脳・心血管イベントの多くは血管の動脈硬化性変化を基盤としている．例えば，血栓性疾患（アテローム血栓症）では慢性炎症病態を基盤とした動脈硬化巣の形成と，それに引き続いて起こる，粥腫（アテローム）の破綻が病態形成に重要である．破綻部位においては，血小板は活性化され，血小板血栓が形

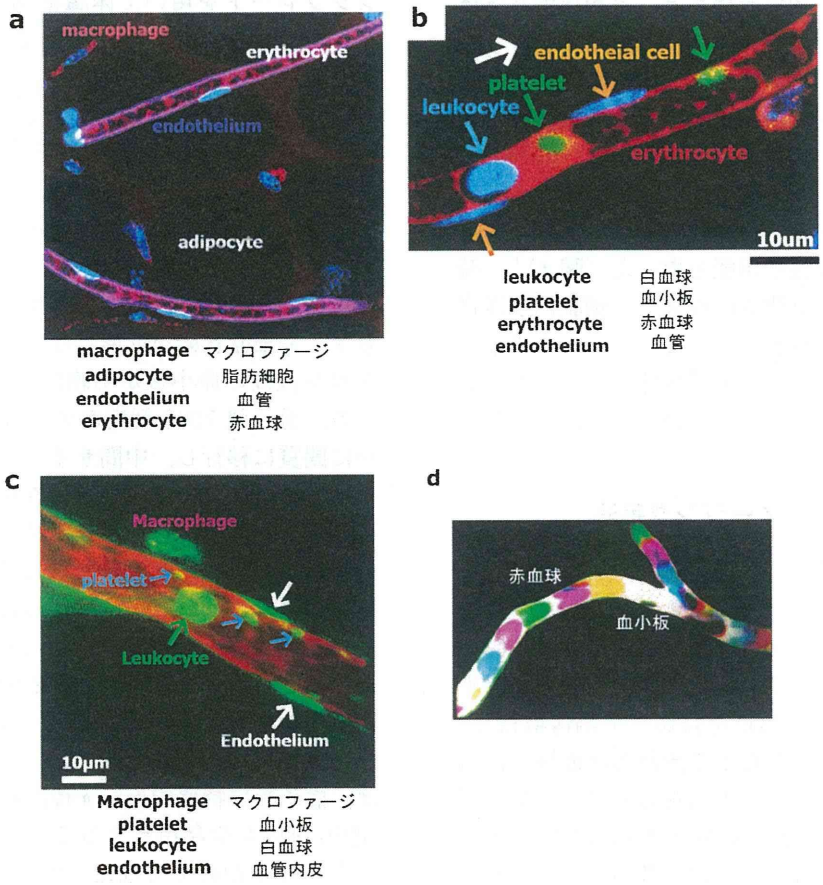

図1　「生体イメージング」でみる体内の細胞動態

「生体イメージング」では手に取るように組織微小循環における生体内の各種細胞の動きが分かる．実験手法詳細については本文中参照．白血球，赤血球，血小板，血管内皮，マクロファージを特異的に染色し，マルチカラーでそれぞれの細胞を特異的に可視化することが可能である．(**d**) のみ連続画像．

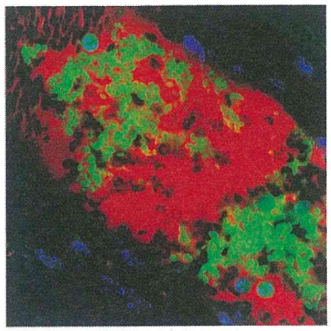

図2　生体内における血栓形成過程

レーザー照射により誘発された微小血栓の形成過程．生体イメージングとレーザー傷害を組み合わせることにより，腸間膜の毛細血管において，血栓を誘発し，血栓形成に寄与する単一血小板を可視化することが可能になった．レーザー照射により血小板血栓が発達している．

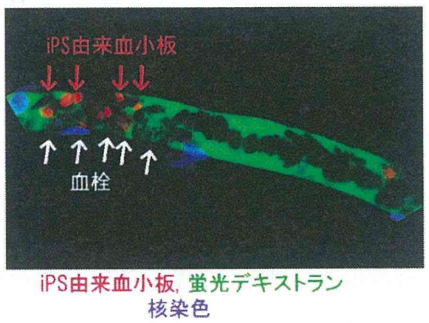

図3　生体内におけるiPS由来人工血小板の血栓形成過程

レーザー照射により誘発されたiPS由来人工血小板の血栓形成過程．
20秒のレーザー照射により人工血小板を含む血小板血栓が発達し血管径が狭小化している．

成される他，凝固系も病態に関与する．しかし，動脈硬化巣の破綻は偶発的かつ高速に進行する病態であり，実験的にこれらを *ex vivo*, *in vitro* で再現することは不可能であった．実際に，これら一連の過程には血小板のみならず，各種炎症性細胞，血管内皮細胞とその障害，局所の血流動態変化（血流とずり応力）が関わっている．このような多細胞からなる複雑病変とそのダイナミクスが血栓性病態の本質であり，これらを生体内で検討する手法が，病態理解の上で求められている．その検討を可能にしたのが我々の開発した「生体分子イメージング」手法である．

血小板をFITC-デキストラン及び抗CD41抗体により可視化したところ，定常状態においては，細動脈・静脈では主に血管壁近傍に沿って血小板は運動していた．一方，流速の遅い毛細血管のレベルでは，血小板は血管内皮と相互作用して「stop and go」を繰り返しており，血流に乗って回転運動している様が可視化された．さらに，レーザー照射・傷害と組み合わせることで血栓形成を誘発し，生体内での単一血小板を捉えながら，血栓形成のメカニズムの詳細が可視化された（**図2**）[2) 3)]．

我々は，レーザー傷害によるROS産生を伴う血栓形成モデルと生体イメージングを組み合わせ，血小板機能に異常を来す各種遺伝子改変動物における血栓形成過程を観察し，生体内での血小板機能との関係を明らかにした．我々のモデルでは楕円形を伴った血小板のみが血栓形成しており，一方，血管内皮の構築は保たれていた．炎症性サイトカインのノックアウトマウス，キメラマウスの解析の結果，TNF-αをはじめとする炎症性サイトカインが，ROS刺激下でのvWF因子の血管内皮表面への表出に関わっていることが明らかになった．さらに，IL-1，IL-6等の因子も血栓性を促進しており，これらの炎症性サイトカインは血管内皮に作用し，インテグリンシグナルと協同して，血栓の安定化に寄与していた．従来，炎症と血栓については多様な報告によりその関連が示唆されていたが，本解析により血栓形成過程のうち，血管内皮における炎症性サイトカインのシグナリングが血栓形成に関わっていることが示された．

我々の血栓形成モデルでは，まずレーザー照射により活性酸素の産生が誘発されて血管内皮に血小板が付着する．活性酸素は血管内皮細胞に直接働き，パイエル小体中のvon Willebrand因子を，細胞膜表面上に移動させる．一方，活性酸素は血小板にも直接作用し，P-selectin，GPIIbIIIaといった機能蛋白が血小板表面に誘導される．その結果，血管内皮のvon Willebrand因子と血小板表面のGPIbが結合し，血栓が誘発される．その後，血小板はその数を増やし積み上り，血管内腔を狭小化し，血液の流速は遅くなる．最終的には，赤血球，もしくは，白血球により血管は閉塞する．我々のモデルが特徴的なのは，血栓形成の全過程が数十秒で終わり，時間的に経過が極めて早いことと，画像が高解像度であることである．本モデルではレーザー照射後に血栓形成に寄与した血小板数を数えることによって血栓形成能を明確に定量可能である．従来の頸動脈に対する塩化鉄傷害モデルにおける血栓による閉塞時間とも強い相関を示しており，生体内の血小板機能を極めて鋭敏に反映していると考えられる．それだけでなく，従来の止血時間の計測では分からなかった，血栓形成の素過程が可視化されており，遺伝子改変の効果がどの過程に影響を及ぼしているかを明らかにすることができる．

我々は本手法を用い，Lnkというアダプター蛋白に注目して実験を進めた．Lnkは血球系幹細胞の維持に重要な蛋白であるが，巨核球・血小板にも発現しているが，その機能は不明であった．興味深いことに，Lnkの欠損した遺伝子改変動物では，流血中の末梢血小板数が野生型の5倍になるにも関わらず血栓性を示さず，むしろ止血時間が延長しており，Lnkの欠損が血小板機能に影響をもたらしていると考えた．骨髄移植を行い作成したLnkキメラマウスを用い，生体イメージングにより血栓形成過程を観察したところ，血球系でのみLnkが欠損したLnkキメラマウスではレーザー傷害により血小板は一過性に血管内皮に付着するものの，血栓は安定化せず血流に崩され，血小板血栓の発達が阻害されているさまが可視化された．すなわち，Lnkが血小板血栓の安定化に寄与していることが示された．分子生物学的機序としてはリン酸化したLnkが，C-Src，Fynと協同してインテグリンのシグナリングに関与してい

た．以上より，Lnkが生体内血栓の形成・安定化に寄与していることが明確に示された．

さらにLnkの遺伝子変異がヒトにおいては，多血症・血小板無力症や骨髄増殖性疾患を引き起こすことも報告されている．多血症では血小板数は増加するものの，血小板機能は低下していることが多く，今回，Lnkノックアウトマウスでみられた表現型にきわめて近いと言え，Lnkの血小板機能における重要性がマウスだけでなく，ヒトにおいても示されている．

今後は，さらに様々な血小板機能に異常を来す遺伝子改変動物における血栓形成過程・血小板動態を観察することにより，「生体内の血栓形成の各過程における遺伝子・物質の関与」が明らかになると思われる．

5. iPS由来人工血小板の体内イメージング

近年の，多能性幹細胞（ES, iPS）の研究の進歩により，細胞療法を含む再生医学での広い範囲での臨床応用が期待されている．しかし，これらの幹細胞を用いた基礎研究を臨床現場に繋げるためには，*in vitro*での知見をヒトを対象とした研究に応用する前に，実際に試験管内で作成した細胞が，実際の個体（マウス及び大動物）の中でどのように機能しているか，どのように病変に働くかを明らかにすることは必須である．しかし，今までこれらiPS由来の分化誘導細胞の体内での細胞動態を検討する手法は存在しなかった．我々は，京都大学iPS細胞研究所江藤教授チームとの共同研究の結果，iPS細胞を誘導するのに必要な山中四因子の中のc-Mycの発現をコントロールすることにより，飛躍的かつ効率的に，ヒトiPS由来の人工血小板を作成する手法を確立した．我々は生体イメージングを用いて，こうして得られたヒトiPS由来血小板の体内動態の可視化を行った．観察に用いた免疫不全マウス（NOGマウス）の体内では，iPS由来人工血小板の細胞動態が捉えられた（**図3**）．iPS由来血小板がマウス体内を循環しているだけでなく，レーザー傷害により誘発された血栓形成部位においてはホスト血小板とiPS由来血小板が相互作用しながら血栓を形成するさまが観察された．つまり，「人工血小板は体内を循環し，血栓も作る」ことが証明されたわけである．このように，本イメージ手法はiPS分化誘導細胞を用いた細胞療法の臨床応用に向けて，安全性・有用性を評価する上できわめて有用性が高い手法と言える[4]．さらに，最近では，人工血小板の作成を飛躍的に改善する分子メカニズムがより明らかになりつつあり，臨床応用も近いと考えられる．

6. おわりに　次世代のイメージング　深部を照らす機能イメージング

我々は今まで主にニポウ式レーザー共焦点，一光子励起の組み合わせで画像取得を行ってきた．しかし，深部臓器・臓器内部の構造に関しては可視化できず，遺伝子機能も不明であった．生体の各種病態下での細胞連関・情報伝達異常をより明らかにするためには，形態と機能とを組み合わせた深部の光イメージングが今後必要になると考えられる．例えば，遺伝子改変動物を用いた遺伝子機能の光による解析を，二光子フェムト秒レーザーと高速スキャニング共焦点システムで行うというものであり，既に多くの生体内深部の知見が得られている．二光子励起による生体イメージングについては，脳組織を用いたイメージングが先行し，それ以外の臓器での知見についてはあまり研究されてこなかったのも実情である．しかし，今後は光学機器の改良に伴う画像の改善・操作性の改善・扱いやすさ使いやすさの向上，顕微鏡システムの価格の一般化，光学プローブの開発改良，が総合的に進むと考えられ，初心者の研究者でも，これらの手法が今後可能になると考えている．

Disclosure of Conflict of Interest

The author indicated no potential conflict of interest.

文　献

1) Nishimura S, Manabe I, Nagasaki M, Seo K, Yamashita H, Hosoya Y, Ohsugi M, Tobe K, Kadowaki T, Nagai R, & Sugiura S：*In vivo* imaging in mice reveals local cell dynamics and inflammation in obese adipose tissue. J Clin Invest **118**(2)：710-721, 2008.
2) Nishimura S, Manabe I, Nagasaki M, Kakuta S, Iwakura Y, Takayama N, Ooehara J, Otsu M, Kamiya A, Petrich B, Urano T, Kadono T, Sato S, Aiba A, Yamashita H, Sugiura S, Kadowaki

T, Nakauchi H, Eto K, Nagai R : *In vivo* imaging visualizes discoid platelet aggregations without endothelium disruption and implicates contribution of inflammatory cytokine and integrin signaling. Blood **119**(8) : e45-56, 2012.
3) Nishimura S, Takizawa H, Takayama N, Oda A, Nishikii H, Morita Y, Kakinuma S, Yamazaki S, Okamura S, Tamura N, Goto S, Sawaguchi A, Manabe I, Takatsu K, Nakauchi H, Takaki S, Eto K : Lnk/Sh2b3 regulates integrin alpha-IIb-beta3 outside-in signaling in platelets leading to stabilization of developing thrombus *in vivo*. J Clin Invest **120**(1) : 179-190, 2010.
4) Takayama N, Nishimura S, Nakamura S, Shimizu T, Ohnishi R, Endo H, Yamaguchi T, Otsu M, Nishimura K, Nakanishi M, Sawaguchi A, Nagai R, Takahashi K, Yamanaka S, Nakauchi H, Eto K : Transient activation of c-MYC expression is critifal for efficient platelet generation from human induced pluripotent stem cells. J Exp Med **207**(13) : 2817-2830, 2010.

genesis 51:763-776 (2013)

ARTICLE

DNA Methylation Profiles Provide a Viable Index for Porcine Pluripotent Stem Cells

Yoshikazu Arai,[1] Jun Ohgane,[2]* Shuh-hei Fujishiro,[3] Kazuaki Nakano,[1] Hitomi Matsunari,[1,4] Masahito Watanabe,[1,4] Kazuhiro Umeyama,[1,4] Dai Azuma,[2] Naomi Uchida,[2] Nozomu Sakamoto,[2] Tomohiro Makino,[2] Shintaro Yagi,[5] Kunio Shiota,[5] Yutaka Hanazono,[3,6] and Hiroshi Nagashima[1,4]*

[1]Department of Life Sciences, Laboratory of Developmental Engineering, School of Agriculture, Meiji University, Kanagawa, Japan

[2]Department of Life Sciences, Laboratory of Genomic Function Engineering, School of Agriculture, Meiji University, Kanagawa, Japan

[3]Division of Regenerative Medicine, Center for Molecular Medicine, Jichi Medical University, Tochigi, Japan

[4]Meiji University International Institute for Bio-Resource Research (MUIIBR), Kanagawa, Japan

[5]Laboratory of Cellular Biochemistry, Animal Resource Sciences/Veterinary Medical Sciences, The University of Tokyo, Tokyo, Japan

[6]CREST, Japan Science and Technology Agency, Tokyo, Japan

Received 18 December 2012; Revised 25 July 2013; Accepted 27 July 2013

Summary: Porcine induced pluripotent stem cells (iPSCs) provide useful information for translational research. The quality of iPSCs can be assessed by their ability to differentiate into various cell types after chimera formation. However, analysis of chimera formation in pigs is a labor-intensive and costly process, necessitating a simple evaluation method for porcine iPSCs. Our previous study identified mouse embryonic stem cell (ESC)-specific hypomethylated loci (EShypo-T-DMRs), and, in this study, 36 genes selected from these were used to evaluate porcine iPSC lines. Based on the methylation profiles of the 36 genes, the iPSC line, Porco Rosso-4, was found closest to mouse pluripotent stem cells among 5 porcine iPSCs. Moreover, Porco Rosso-4 more efficiently contributed to the inner cell mass (ICM) of blastocysts than the iPSC line showing the lowest reprogramming of the 36 genes (Porco Rosso-622-14), indicating that the DNA methylation profile correlates with efficiency of ICM contribution. Furthermore, factors known to enhance iPSC quality (serum-free medium with PD0325901 and CHIR99021) improved the methylation status at the 36 genes. Thus, the DNA methylation profile of these 36 genes is a viable index for evaluation of porcine iPSCs. genesis 51:763–776. © 2013 Wiley Periodicals, Inc.

Key words: epigenetics; induced pluripotent stem cells; translational research

INTRODUCTION

The use of induced pluripotent stem cells (iPSCs) is expected to dramatically accelerate advances in medical care (Okita and Yamanaka, 2011; Takahashi and Yamanaka, 2006; Takahashi *et al.*, 2007). In particular, iPSCs may offer novel therapies for previously intractable

Additional Supporting Information may be found in the online version of this article.

*Correspondence to: Jun Ohgane, Laboratory of Genomic Function Engineering, Department of Life Sciences, School of Agriculture, Meiji University, 1-1-1 Higashimita, Tama, Kawasaki 214-8571, Japan (or) Hiroshi Nagashima, Laboratory of Developmental Engineering, Department of Life Sciences, School of Agriculture, Meiji University, 1-1-1 Higashimita, Tama, Kawasaki 214-8571, Japan. E-mail: johgane@meiji.ac.jp (or) hnagas@isc.meiji.ac.jp

Contract grant sponsor: Core Research for Evolutional Science and Technology (CREST) of the Japan Science and Technology Agency (to Y.H. and H.N.), Contract grant sponsor: Meiji University International Institute for Bio-Resource Research (MUIIBR) (to H.N.); Contract grant sponsor: Japan Society for the Promotion of Science (JSPS) Grant-in-Aid for Young Scientists (B) (to J.O.), Contract grant sponsor: Research Project Grant (B) by Institute of Science and Technology Meiji University (to J.O.); Contract grant sponsor: Meiji University Grant for Research by Young Scientist (to Y.A.)

Published online 30 August 2013 in Wiley Online Library (wileyonlinelibrary.com).

DOI: 10.1002/dvg.22423

conditions, and a wide range of possible applications has been investigated including exploration of the pathogenic mechanisms of refractory diseases and the development of new drugs (Ebert *et al.*, 2009; Imaizumi *et al.*, 2012; Inoue and Yamanaka, 2011), cell therapy (Montserrat *et al.*, 2011; Zhou *et al.*, 2011), production of organs and tissues (Kobayashi *et al.*, 2010; Usui *et al.*, 2012), and generation of germ cells (Hayashi *et al.*, 2011, 2012).

Before iPSCs can be used for clinical applications, it is essential that appropriate experiments using animal models are carried out to ensure their effectiveness and safety. In addition to the use of standard laboratory animals such as rodents, investigation of larger animal species, with closer physiological resemblance to humans, will significantly benefit translational research. The pig is one such species and has many similarities in anatomy and physiology to humans (van der Spoel *et al.*, 2011; Zhao and Prather, 2011); pigs have often been used in biomedical studies as a large experimental model, which can produce data that can be easily applied to humans (Lunney, 2007; Petters, 1994; Prather *et al.*, 2003). Therefore, the generation and evaluation of porcine iPSCs will provide useful information that could help promote clinical application of human iPSCs (Ezashi *et al.*, 2009; Fujishiro *et al.*, 2013; Montserrat *et al.*, 2011; West *et al.*, 2010; Wu *et al.*, 2009).

The pluripotency of porcine iPSCs can be evaluated by determining their ability to form chimeras (Fujishiro *et al.*, 2013; West *et al.*, 2010). However, the production of chimeric fetuses and piglets is a labor-intensive and costly process that requires embryo manipulation and transfer. Indeed, few studies have used chimera-forming ability as a means of confirming the pluripotency of porcine iPSCs (Fujishiro *et al.*, 2013; West *et al.*, 2010, 2011). Therefore, it is essential to develop new methods, either for evaluating the pluripotency of porcine iPSCs, or for pre-screening iPSC lines for use in chimera formation experiments.

Epigenetic regulation, including DNA methylation and histone modifications, is fundamental to tissue- and/or cell-type specific gene expression (Golob *et al.*, 2008; Ikegami *et al.*, 2009; Lieb *et al.*, 2006; Shiota *et al.*, 2004). There are a large number of tissue-dependent differentially methylated regions (T-DMRs) in the mammalian genome (Shiota *et al.*, 2002; Yagi *et al.*, 2008). The DNA methylation status of T-DMRs is determined during embryonic development, and the DNA methylation profile of T-DMRs is distinctive in each cell type (Sakamoto *et al.*, 2007; Shiota *et al.*, 2002). Mouse ESCs, which are known to be pluripotent stem cells, exhibit unique DNA methylation profiles at T-DMRs. Genes involved in the establishment and maintenance of the pluripotent state, including *Oct3/4* (*Pou5f1*), are hypomethylated in mouse ESCs (Hattori *et al.*, 2004; Imamura *et al.*, 2006). Genome-wide DNA methylation analyses have identified several hundred mouse ESC-specifically hypomethylated T-DMRs (EShypo-T-DMRs; Sato *et al.*, 2010). Furthermore, it has been shown that the DNA methylation profiles of EShypo-T-DMRs in mouse iPSCs with a high efficiency of chimera formation are similar to those of ESCs (Aoi *et al.*, 2008; Sato *et al.*, 2010). These results indicate that the DNA methylation profile of EShypo-T-DMRs provide a viable index for screening high-quality iPSCs.

We recently generated naïve-like porcine iPSC lines using the four Yamanaka factors (*Oct3/4*, *Sox2*, *Klf4*, and *c-Myc*; Fujishiro *et al.*, 2013); these factors are also used to generate mouse iPSCs. These porcine iPSC lines exhibit LIF-dependent proliferation abilities similar to those of mouse ESCs/iPSCs (Fujishiro *et al.*, 2013); however, the lines also show different characteristics.

In this study, we sought to determine whether the DNA methylation index for mouse EShypo-T-DMRs could be used to evaluate porcine iPSC lines. If this approach is feasible for the evaluation of porcine iPSCs, then the same strategy could be applied to quality enhancement of iPSCs from a wide range of domesticated animal species and ultimately for human iPSCs.

RESULTS

DNA Methylation Profile of 36 Genes Known to be Specifically Hypomethylated in Mouse ESCs in Porcine iPSCs

To analyze DNA methylation profiles of porcine iPSCs, we selected 36 genes that are hypomethylated specifically in mouse ESCs (EShypo-T-DMRs; Sato *et al.*, 2010). The 36-gene set was categorized into three groups; those targeted by Oct3/4 (Oct3/4-targets); Klf4, Sox2, or c-Myc (KSM-targets); and genes, which are not targets of these four factors (non-targets; Fig. 1a). In the course of iPSC establishment, activation of target genes of the four Yamanaka factors is required after introduction into somatic cells. Among the four factors, Oct3/4 is of utmost importance since iPSC lines have not been established without *Oct3/4* introduction to date. Thus, target genes of Oct3/4, such as *Sall4* (Tsubooka *et al.*, 2009), are thought to have crucial roles in iPSC establishment, and the Oct3/4 target genes (Oct3/4-targets) were separated from the target genes of the other three Yamanaka factors (KSM-targets). Although "non-targets" are genes that are not directly bound by the four Yamanaka factors, their methylation levels in mouse ESCs were lower than those in differentiated tissues/cells (Sato *et al.*, 2010), suggesting that the DNA methylation statuses of non-targets can also be useful as an index for evaluation of porcine iPSCs. The classification of target genes was based on ChIP-seq data for several transcription factors, including the four Yamanaka factors (Chen *et al.*, 2008). We initially selected 56

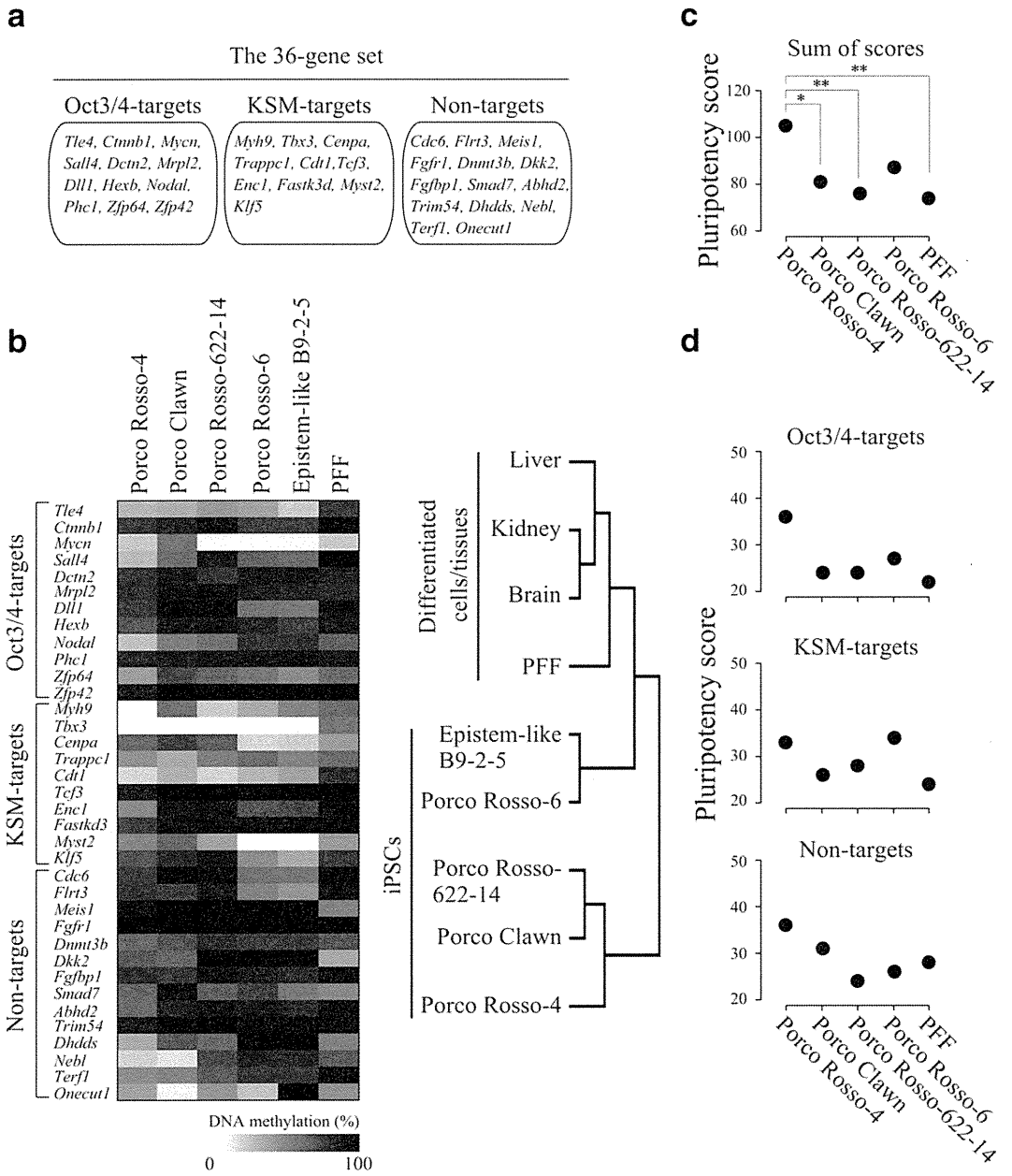

FIG. 1. DNA methylation profiles of porcine iPSCs. (**a**) The 36-gene set analyzed for DNA methylation profiling of porcine iPSCs. The genes were retrieved from EShypo-T-DMRs previously determined in mouse ESCs, and were categorized into three groups: Oct3/4-targets, KSM-targets, and non-targets. (**b**) DNA methylation status of the 36-gene set in five iPSC lines (Porco Rosso-4, Epistem-like B9-2-5, Porco Rosso-6, Porco Rosso-622-14, and Porco Clawn) and porcine fetal fibroblast (PFF) by COBRA assay. The methylation level is represented as a heatmap (left panel). Based on the methylation level determined by COBRA assay, differentiated cell or tissues (brain, liver, kidney, and PFF) and five porcine iPSC lines were clustered according to the similarity of their DNA methylation profiles at the 36 selected genes using the Euclidean distance (right panel). (**c**) Sum of pluripotency scores of the 36 genes for porcine naïve-like iPSCs and PFF. Depending on percentage difference in methylation levels between blastocysts and iPSCs, pluripotency scores for each gene were classified into five categories: $< 20\%$, 20–40%, 40–60%, 60–80%, or $> 80\%$, with pluripotency scores of 5, 4, 3, 2, or 1, respectively. Total scores of the 36-gene set are plotted. Statistical comparison was performed by Wilcoxon test. $^{*}P < 0.05$; $^{**}P < 0.01$. (**d**) Pluripotency scores of porcine iPSCs and PFF for each of the three gene-groups. Total scores of the genes belonging to each group (Oct3/4-targets, KSM-targets, and non-targets) are plotted.

porcine genes orthologous to mouse genes with EShypo-T-DMRs, whose DNA methylation levels were low in mouse ESCs but 30% or more higher in differentiated tissues/cells (Sato *et al.*, 2010). However, 16 of these were found to be hypomethylated in porcine somatic tissues, and further, four genes were hypermethylated in porcine blastocysts, consisting of pluripotent cells (Supporting Information Fig. 1). Therefore, these 20 genes were excluded, and the remaining 36 were used for DNA methylation analyses. Among these 36 genes, several are known to be hypomethylated in mouse ESCs, but to be in a poised state of transcriptional activation, rather than actively expressed. This type of epigenetic regulation has been reported in H3K4me3/H3K27me3-enriched bivalent regions (Meissner *et al.*, 2008; Xu *et al.*, 2007).

We performed DNA methylation analyses of the 36 selected genes in five porcine iPSC lines; Porco Rosso-4, −6, −622-14, Epistem-like B9-2-5, and Porco Clawn. Epistem-like B9-2-5 was cultured in typical non-mouse ESC/iPSC media containing bFGF (Fujishiro *et al.*, 2013), and its colony shape and gene expression patterns were similar to those of mouse epiblast stem cells (EpiSCs; Brons *et al.*, 2007; Tesar *et al.*, 2007). The other four cell lines were cultured with porcine LIF, and their colony shape was similar to that of mouse ESCs (Fujishiro *et al.*, 2013). DNA methylation levels of the 36 genes were examined by combined bisulfite restriction analysis (COBRA) assay (Xiong and Laird, 1997) in iPSCs and porcine fetal fibroblast (PFF) used to produce the iPSC lines (Fig. 1b, left panel). Hierarchical clustering of DNA methylation status was performed on the basis of the 36-gene set for somatic cells/tissues and iPSC lines (Fig. 1b, right panel). Somatic tissues (brain, liver, and kidney) and PFF clustered together, whereas the five iPSC lines clustered separately, indicating that the DNA methylation profile of the 36-gene set could distinguish between differentiated cells/tissues and iPSCs.

Next, we determined a "Pluripotency score" based on comparison of methylation levels of the 36 genes between blastocysts consisting of pluripotent cells and the four naïve-like iPSC lines. Since Epistem-like B9-2-5 is distinguishable from naïve-like iPSC lines based on the mouse EpiSC-like colony shape and bFGF-dependent proliferation (Fujishiro *et al.*, 2013), Epistem-like B9-2-5 was excluded in the following experiments. Scoring was performed for each gene, and the sum of the scores of the 36 genes was plotted (Fig. 1c). In this way, high pluripotency scores are awarded to iPSC lines with DNA methylation profiles close to those of pluripotent cells. Among the four iPSC lines examined, Porco Rosso-4 showed the highest pluripotency score, which was statistically significant when compared with PFF, Porco Rosso-622-14, and Porco Clawn. We further examined the pluripotency score depending on the gene groups (Oct3/4-targets, KSM-targets, or non-targets; Fig. 1d). The Oct3/4-target genes had higher pluripotency scores in the Porco Rosso-4 cell line (36) than the other three cell lines and PFF (22–27). This tendency was also observed for non-target genes. By contrast, the score of KSM-target genes in Porco Rosso-4 was similar to that of Porco Rosso-6. Thus, among the four iPSC lines examined, the DNA methylation profile of Porco Rosso-4 is most similar to that of pluripotent cells. This was consistent with the results of the hierarchical clustering analysis, where the Porco Rosso-4 line was separate from the Epistem-like B9-2-5 line.

We confirmed the DNA methylation status of six gene loci (*Ctnnb1*, *Sall4*, *Tle4*, *Dll1*, *Enc1*, and *Nebl*), whose DNA methylation level was clearly different among the examined iPSC lines (Fig. 1b, left panel), by bisulfite sequencing. All 6 gene loci were hypermethylated in PFF and liver, whereas hypomethylated status was observed in blastocysts (Fig. 2). DNA methylation levels of the Oct3/4-target genes, *Ctnnb1* and *Sall4*, were 24 and 2%, respectively in the Porco Rosso-4 line, which had the highest pluripotency score among the four iPSC lines. However, Porco Rosso-622-14, which had the lowest pluripotency score, exhibited hypermethylation at the *Ctnnb1* (65%) and *Sall4* (61%) loci. This indicates that *Ctnnb1* and *Sall4* are highly demethylated in Porco Rosso-4 but not in Porco Rosso-622-14 cells. At the other four gene loci, partial demethylation was also observed in Porco Rosso-4 but not Porco Rosso-622-14. These bisulfite sequencing results confirm that, in Porco Rosso-4 iPSC line, DNA methylation patterns of the 6 genes, we analyzed changed to the expected direction as pluripotent cells, and Oct3/4-target genes, *Sall4* and *Ctnnb1*, especially underwent demethylation within the entire sequenced regions in the majority of the cell population.

Contribution of Porcine iPSCs to the Inner Cell Mass (ICM) of Blastocysts

Established iPSC lines are intended for use in transplantation and complementation experiments. Considering that the naïve-like iPSC lines do not differ greatly in terms of morphology and marker gene expression (Fujishiro *et al.*, 2013), it is more appropriate to select candidate iPSC lines using different indices. We next investigated contribution of the iPSC lines to the ICM of blastocysts using the aggregation method (Fig. 3a). We performed two independent experiments (Exps. 1 and 2), and found that Porco Rosso-4 cells contributed better to the ICM compared with Porco Rosso-622-14 in both experiments (Fig. 3b). In Exps. 1 and 2, the number of embryos that exhibited ICM contribution of iPSCs statistically differed between Porco Rosso-4 (14/57, 24.6%) and Porco Rosso-622-14 (2/51, 3.9%; Fig. 3c). The sum of pluripotency scores (105) for the three gene groups (Oct3/4-targets, KSM-targets, and non-targets) for Porco

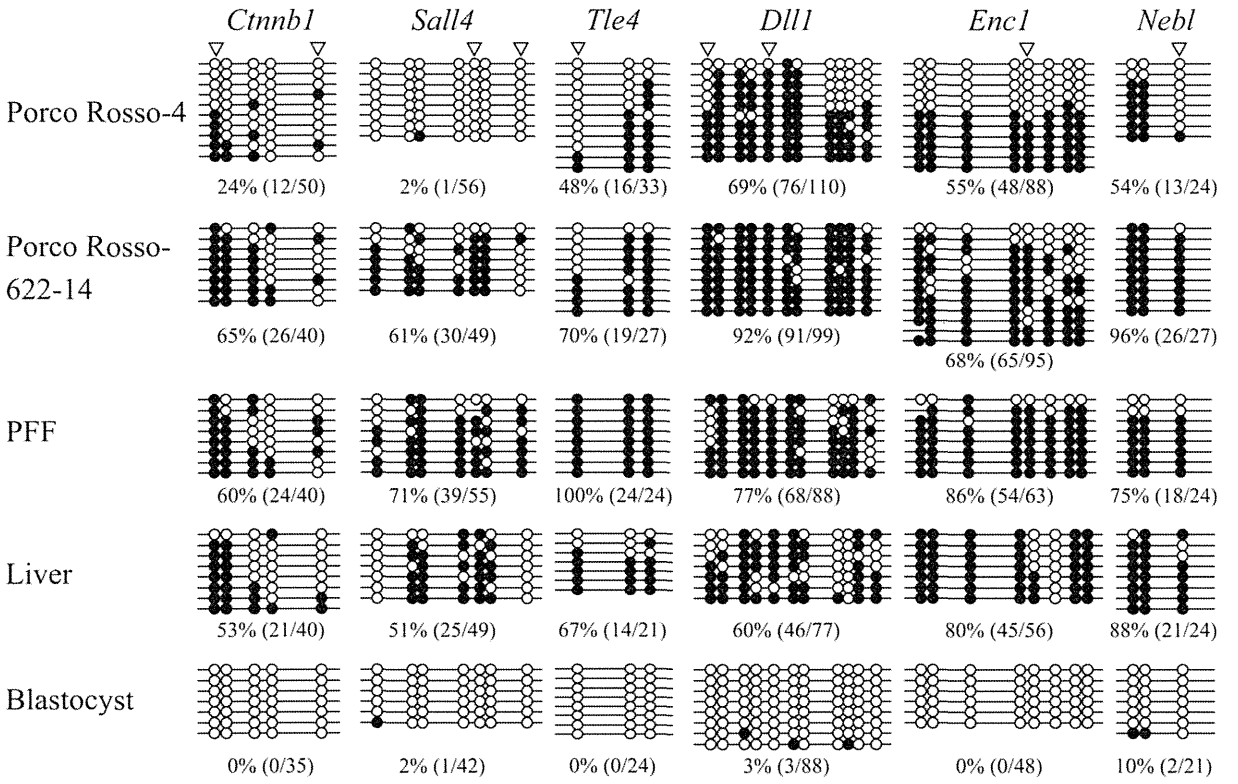

FIG. 2. DNA methylation status of EShypo-T-DMRs in iPSCs (Porco Rosso-4 and Porco Rosso-622-14) analyzed by sodium bisulfite sequencing. Open and closed circles indicate unmethylated and methylated CpG dinucleotides, respectively. Arrowheads indicate CpG sites analyzed by COBRA assay. The methylation level (%) was based on the methylated CpGs/all examined CpGs.

Rosso-4 was higher than that of Porco Rosso-622-14 (76), indicating that a higher pluripotency score coincides with higher efficiency of incorporation of iPSCs into the ICM. Thus, the pluripotency score based on the DNA methylation status of the 36 genes provides a feasible index for evaluating porcine iPSCs.

DNA Methylation Analysis in huKO-Negative Cells

We previously reported that approximately 5% of the cell population in Porco Rosso-4 became negative for humanized Kusabira-Orange (huKO) fluorescence (huKO-negative cells), and their characteristics were closer to those of the expected pluripotent cells (Fujishiro *et al.*, 2013). This implies that high-quality porcine iPSCs were enriched in huKO-negative fraction. To confirm whether the DNA methylation profile of EShypo-T-DMRs is a useful index for screening porcine iPSCs, we analyzed the DNA methylation status of huKO-negative cells. The huKO-negative cells in Porco Rosso-4 were collected by cell sorting, together with cells with high expression of huKO (huKO positive; Fig. 4a). EShypo-T-DMRs (*Dll1* and *Enc1*) were analyzed by bisulfite sequencing, because approximately half of the sequenced clones exhibited obvious hypomethylation in Porco Rosso-4 (Figs. 2 and 4), suggesting that Porco Rosso-4 contains a certain proportion of the cells properly demethylated at these two loci. Based on the bisulfite sequence data (Fig. 4b), the percentage of the cells hypomethylated at these two loci in Porco Rosso-4 was calculated on the basis of the number of unmethylated CpGs in the sequenced clones before and after sorting (Fig. 4c). Before sorting, the percentages of hypomethylated cells at the *Dll1* and *Enc1* loci were estimated as 36% and 50%, respectively. In huKO-negative fraction, 67–80% of the cells were considered as hypomethylated, whereas the proportion of hypomethylated cells in the huKO-positive fraction were lower than that of the cells before sorting, indicating that huKO-negative cells were hypomethylated at these EShypo-T-DMRs as expected from the DNA methylation patterns in mouse ESCs. Thus, the DNA methylation profile based on the EShypo-T-DMRs reflects the characteristics of the expected cells.

Improvement of Pluripotency Scores of Porcine iPSCs by SF + 2i Treatment

It is known that treatment with two signal-transduction inhibitors (2i) of PD0325901, an inhibitor of mitogen-activated protein kinase/extracellular signal-

a

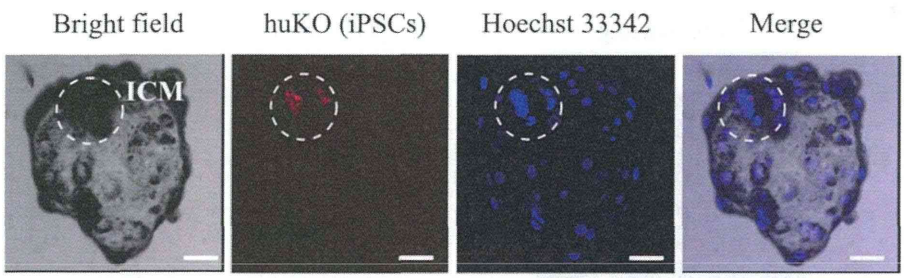

b

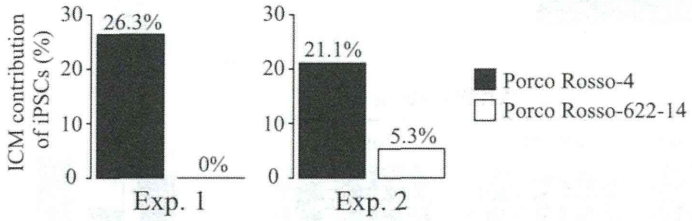

c

Donor cell	n	Developed to blastocyst	Number of * blastocysts analyzed	Contribution to ** ICM	Sum of *** pluripotency score (/180)
Porco Rosso-4	345	280/345 (81.2%)	57	14/57[a] (24.6%)	105
Porco Rosso-622-14	146	123/146 (84.2%)	51	2/51[b] (3.9%)	76
ICM	50	46/50 (92.0%)	46	37/46 (80.4%)	–

ab, $p<0.01$ (chi-square test)
*, The other blastocysts were used for different experiments.
**, Porco Rosso-4, n=38 (Exp. 1) and n=19 (Exp. 2). Porco Rosso-622-14, n=13 (Exp. 1) and n=38 (Exp. 2).
***, Pluripotency score was calculated only for iPSCs.

FIG. 3. Contribution of iPSCs to the ICM of blastocysts. (**a**) Porcine iPSCs (Porco Rosso-4 and Porco Rosso-622-14) were aggregated with porcine parthenogenetic 4- to 8-cell-, or morula-stage embryos. After in vitro culture, contribution of iPSCs to blastocysts was analyzed by fluorescence of the transgene, humanized Kusabira-Orange (huKO). Scale bar = 50 μm. (**b**) The percentage of ICM contribution of Porco Rosso-4 and Porco Rosso-622-14. Aggregation experiments using porcine iPSCs (Porco Rosso-4 and Porco Rosso-622-14) were performed twice independently (Exps. 1 and 2). (**c**) Summary of the contribution of iPSCs to the ICM of blastocysts. Using the ICM cells dissociated from blastocysts as donor cells, most aggregated embryos developed into blastocysts, and donor ICM cells could contribute efficiently to the ICM of the host blastocyst, confirming the contribution of pluripotent cells to the ICM. Statistical comparison was performed by chi-square test.

regulated kinase (ERK) kinase (MEK), and CHIR99021, an inhibitor of GSK3β, is effective for establishment of a naïve state in iPSCs from rodent and human (Buehr *et al.*, 2008; Hanna *et al.*, 2009; Li *et al.*, 2008). Additionally, 2i treatment has been shown to improve the characteristics of porcine iPSCs (Rodríguez *et al.*, 2012). We examined whether the DNA methylation profile of the 36 selected genes is a useful index for evaluation of the changes in characteristics of porcine iPSCs after 2i treatment. We analyzed the DNA methylation status of Porco Clawn cultured in medium with FBS, or in serum-free (SF) or in SF+2i medium, by COBRA assay (Fig. 5a, left panel). Cells treated with 5-aza-2′-deoxycytidine (5-aza-dC), an inhibitor of DNA methyltransferase 1, were also analyzed for DNA methylation status.

In the course of mouse iPSC establishment, promoter regions of pluripotency-related genes, including EShypo-T-DMRs become demethylated (Okita *et al.*, 2007; Sato *et al.*, 2010; Takahashi and Yamanaka, 2006). In this study, we observed that porcine iPSCs cultured under SF conditions exhibited effective demethylation of the Oct3/4-target genes compared with FBS-cultured cells (Fig. 5a, right panel). In addition, the number of demethylated and reprogrammed genes was greatly increased under the SF+2i condition. These tendencies were also observed in the KSM-target and non-target gene groups, suggesting that SF+2i condition induced demethylation of the 36 selected genes. However, 5-aza-dC treatment was not effective, and the number of hypomethylated Oct3/4-target genes